OXFORD
SOT | Society of Toxicology
www.toxsci.oxfordjournals.org
ToxSci 20 Years

TOXICOLOGICAL SCIENCES, 163(2), 2018, 592–608

doi: 10.1093/toxsci/kfy062
Advance Access Publication Date: March 21, 2018
Research Article

# Subchronic Manganese Exposure Impairs Neurogenesis in the Adult Rat Hippocampus

Sherleen Xue-Fu Adamson,* Xubo Shen,* Wendy Jiang,* Vivien Lai,* Xiaoting Wang,[‡,§] Jonathan H. Shannahan,* Jason R. Cannon,[*,†] Jinhui Chen,[‡,§] and Wei Zheng[*,†,1]

*School of Health Sciences and †Purdue Institute for Integrative Neurosciences, Purdue University, West Lafayette, IN 47907; ‡Spinal Cord and Brain Injury Research Group, Stark Neuroscience Research Institute; and §Department of Neurological Surgery, Indiana University School of Medicine, Indianapolis, IN 46202

[1]To whom correspondence should be addressed at School of Health Sciences, Purdue University, 550 Stadium Mall Drive, Room 1169, West Lafayette, IN 47907. Fax: (765) 496-1377. E-mail: wzheng@purdue.edu.

## ABSTRACT

Adult neurogenesis takes place in the brain subventricular zone (SVZ) in the lateral walls of lateral ventricles and subgranular zone (SGZ) in the hippocampal dentate gyrus (HDG), and functions to supply newborn neurons for normal brain functionality. Subchronic Mn exposure is known to disrupt adult neurogenesis in the SVZ. This study was designed to determine whether Mn exposure disturbed neurogenesis within the adult HDG. Adult rats (10 weeks old) received a single dose of bromodeoxyuridine (BrdU) at the end of 4-week Mn exposure to label the proliferating cells. Immunostaining and cell counting data showed that BrdU(+) cells in Mn-exposed HDG were about 37% lower than that in the control ($p < .05$). The majority of BrdU(+) cells were identified as Sox2(+) cells. Another set of adult rats received BrdU injections for 3 consecutive days followed by 2- or 4-week Mn exposure to trace the fate of BrdU-labeled cells in the HDG. The time course studies indicated that Mn exposure significantly reduced the survival rate (54% at 2 weeks and 33% at 4 weeks), as compared with that in the control (80% at 2 weeks and 51% at 4 weeks) ($p < .01$). A significant time-dependent migration of newborn cells from the SGZ toward the granule cell layer was also observed in both control and Mn-exposed HDG. Triple-stained neuroblasts and mature neurons further revealed that Mn exposure significantly inhibited the differentiation of immature neuroblasts into mature neurons in the HDG. Taken together, these observations suggest that subchronic Mn exposure results in a reduced cell proliferation, diminished survival of adult-born neurons, and inhibited overall neurogenesis in the adult HDG. Impaired adult neurogenesis is likely one of the mechanisms contribute to Mn-induced Parkinsonian disorder.

**Key words:** manganese; adult neurogenesis; dentate gyrus; subgranular zone; granule cell layer.

Manganese (Mn) is essential for normal brain development and function (Akai *et al.*, 1990; Aschner and Aschner, 2005; Aschner *et al.*, 2007; Wedler *et al.*, 1982; Wedler and Denman, 1984). However, overexposure to Mn from environmental and occupational sources, or due to disease conditions can cause manganism, a well-recognized neurodegenerative disorder with signs and syndromes that are similar, but not identical to idiopathic Parkinson's disease (Barbeau *et al.*, 1976; Jiang *et al.*, 2006, 2007; Racette *et al.*, 2012). Studies on humans, primates and rodents demonstrate that upon crossing the blood-brain and blood-cerebrospinal fluid barriers, Mn selectively accumulates in the globus pallidus, substantia nigra, and hippocampus (Dietz *et al.*, 2001; Dydak *et al.*, 2011; Fu *et al.*, 2014; Jiang *et al.*, 2007; Lucchini *et al.*, 2000; Robison *et al.*, 2013; Zheng *et al.*, 2009). However, mechanisms by which Mn induces neuropathological and neurochemical alterations remain unclear.

Recent data from this laboratory using synchrotron x-ray fluorescence (XRF) microscopy reveal that the hippocampal dentate gyrus (HDG) and cornus ammonis 3 (CA3) accumulate the highest amount of Mn in Mn-exposed rats

(Robison *et al.*, 2012, 2013). The HDG plays an essential role in regulating brain functions such as learning, memory, cognition, and spatial behavior (Clark *et al.*, 2000; Eichenbaum, 2004; Jonas and Lisman, 2014; Liang *et al.*, 2015; Montaron *et al.*, 2004; Sutherland *et al.*, 1982). During the adulthood, the HDG continuously generate new neurons derived from neural stem/progenitor cells (NSPCs) harbored within the subgranular zone (SGZ), a known active neurogenic niche that functions to create and maintain neurogenesis (Kempermann and Gage, 2000; Ming and Song, 2005). The adult-born NSPCs after exiting the cell cycle are capable of migrating toward the inner layer of the granule cell layer (GCL) and further develop into mature granular neurons (Ming and Song, 2005; Shapiro and Ribak, 2005; Zhao *et al.*, 2006). More specifically, the original NSPCs residing in the SGZ are radial glia-like progenitor cells (type 1) expressing glial fibrillary acid protein (GFAP) and nestin, which remain quiescent under basal physical condition. Once activated by intrinsic or extrinsic stimuli, they can proliferate and become types 2a and 2b precursors, and further develop into type 3 immature neurons. Ultimately, the type 3 cells migrate locally in the GCL and differentiate into mature granule cells (Hodge *et al.*, 2008). Hence, the population of NSPCs is an indispensable source of new neurons for supporting neuroplasticity and granule cell turnover, and compensating the neuronal loss in adult hippocampus.

Excessive Mn deposits in the hippocampus have been associated with neurobehavioral alterations such as impaired spatial learning, memory loss and cognitive deficits in rodents, nonhuman primates and humans (Blecharz-Klin *et al.*, 2012; Bowler *et al.*, 2003, 2006; Carvalho *et al.*, 2014; Fitsanakis *et al.*, 2009; Menezes-Filho *et al.*, 2011; Oner and Sentürk, 1995; Peres *et al.*, 2015; Riojas-Rodríguez *et al.*, 2010; Schneider *et al.*, 2013). For its role in adult neurogenesis, the hippocampus could be a target area where accumulated Mn may impede the neural regeneration and repair owing to the neurogenic activity in the HDG. Recent studies have found that Mn exposure can cause apoptosis in immature granule cells, misguide neuronal migration, increase immature interneurons, and disrupt the epigenetic gene regulation in mouse HDG following Mn exposure (Wang *et al.*, 2012, 2013). However, results by Ohishi *et al.* (2012) have shown that maternal Mn exposure induces a mild and reversible neurogenesis in the HDG of offspring rats. Studies by Kikuchihara *et al.* (2015) report that Mn accumulation in the brain can reduce types 2b and 3 progenitors as well as GABAergic interneurons in Mn-exposed adult mouse HDG. However, none of these studies have employed bromodeoxyuridine (BrdU) or other useful markers to label newborn progenitors and to trace dynamic changes of NSPCs during the entire neurogenesis process, so as to distinguish cell phenotypes at different neurogenic phases and quantify numbers of proliferating, survived, and differentiated adult-born cells in the HDG.

To understand the dynamic changes of NSPCs and their progenies in the adult HDG following Mn exposure, we designed two separate experiments using different BrdU labeling paradigms to trace and analyze the fate of BrdU-labeled newborn cells in the HDG. In experiment 1 (Figure 1A), the proliferating cells in the adult rat HDG were labeled by a single dose of BrdU and quantified within a 4-h time window after subchronic Mn exposure. Experiment 2 (Figure 1B) was performed by pulse-labeling newly generated NSPCs in the HDG with BrdU prior to Mn exposure; these cells were then traced for their survival and differentiation at different exposure time points. Results from these experiments provide the first hand evidence on Mn detrimental effect on various phases of adult hippocampal neurogenesis.

## MATERIALS AND METHODS

*Materials*. Chemical reagents were purchased from the following sources: Rabbit anti-rat DMT1 antibody was obtained from Alpha Diagnostic (San Antonio, CA), mouse monoclonal anti-BrdU antibody from Santa Cruz Biotechnology (Dallas, TX), ProLong Gold antifade reagent, Alexa Fluor 488 goat anti-rabbit IgG (H + L) antibody (Catalog# A11008) and Alexa Fluor 555 goat anti-mouse IgG (H + L) antibody (A21424) from Life Technologies (Carlsbad, CA); rabbit polyclonal anti-Sox2 (Catalog# ab97959), anti-doublecortin (DCX) (ab18723) and anti-NeuN (ab177487) antibodies, and chicken polyclonal anti-glial fibrillary acidic protein (GFAP) antibodies from Abcam (Cambridge, MA); polyclonal rabbit anti-ionizing calcium-binding adaptor molecule 1 (Iba1) antibody (Catalog# WEE4506) from Wako Chemicals USA Inc (Richmond, VA); manganese chloride tetra-hydrate ($MnCl_2{\cdot}4H_2O$) from Fisher scientific (Pittsburgh, PA); Protease Inhibitor Cocktail from Calbiochem (San Diego, CA); paraformaldehyde (PFA) from ACROS Organics (Morris Plains, NJ); bovine serum albumin (BSA) from AMRESCO (Solon, OH); and normal goat serum from Jackson ImmunoResearch Laboratories (West Grove, PA). All reagents were of analytical grade, HPLC grade, or the best available pharmaceutical grade.

*Animals and Mn administration*. Male Sprague-Dawley rats were purchased from Harlan Sprague Dawley Inc. (Indianapolis, IN). At the time of use, the rats were 10-week old weighing 220–250 g. Upon arrival, rats were housed in a temperature-controlled, 12/12-h light/dark cycle room and allowed to acclimate for one week prior to experimentation. They had free access to deionized water and pellet Purina semipurified rat chow (Purina Mills Test Diest, 5755C; Purina Mills, Richmond, Inc). The study was conducted in compliance with standard animal use practices and approved by the Animal Care and Use Committee of Purdue University.

$MnCl_2{\cdot}4H_2O$ was dissolved in sterile saline. Rats received intraperitoneal (IP) injections of $MnCl_2$ solution (1 ml/kg body weight) at a concentration of 6 mg Mn/kg, once daily, 5 days/week for 4 consecutive weeks. This dose regimen was selected based on previous studies from this and other laboratories, which is known to be associated with a significant reduction of succinic dehydrogenase and a significant inhibition of mitochondrial aconitase in rat brain (Seth *et al.*, 1977, 1981; Singh *et al.*, 1974; Zheng *et al.*, 1998, 2000), and that the Mn concentration in the blood after 4-week IP doses reached ~50 μg/l (Fu *et al.*, 2014), which is comparable with blood Mn levels in Mn-exposed rodents through oral doses (O'Neal *et al.*, 2014a) and Mn-exposed human subjects (Crossgrove and Zheng, 2004). In addition, the same dose regimen was found to increase significantly Mn levels in different brain regions, ie, striatum, frontal cortex, hippocampus, choroid plexus, and CSF (Fu *et al.*, 2014, 2015a; O'Neal *et al.*, 2014b). The daily equivalent volume of sterile saline was given to the animals in the control group.

*BrdU administration*. BrdU was administered by IP injection(s) to rats with or without Mn exposure. Two different experimental protocols were designed to investigate the Mn effect on different states of adult neurogenesis, including proliferation, survival, and differentiation, in the HDG. Experiment 1 was designed to evaluate Mn effect on the cell proliferation in the HDG. Rats underwent subchronic Mn exposure as described above. Twenty-four hour after the last Mn dose, rats received a single dose of BrdU (50 mg/kg, IP) and were necropsied 4 h later (Figure 1A). Experiment 2 was designed to determine whether

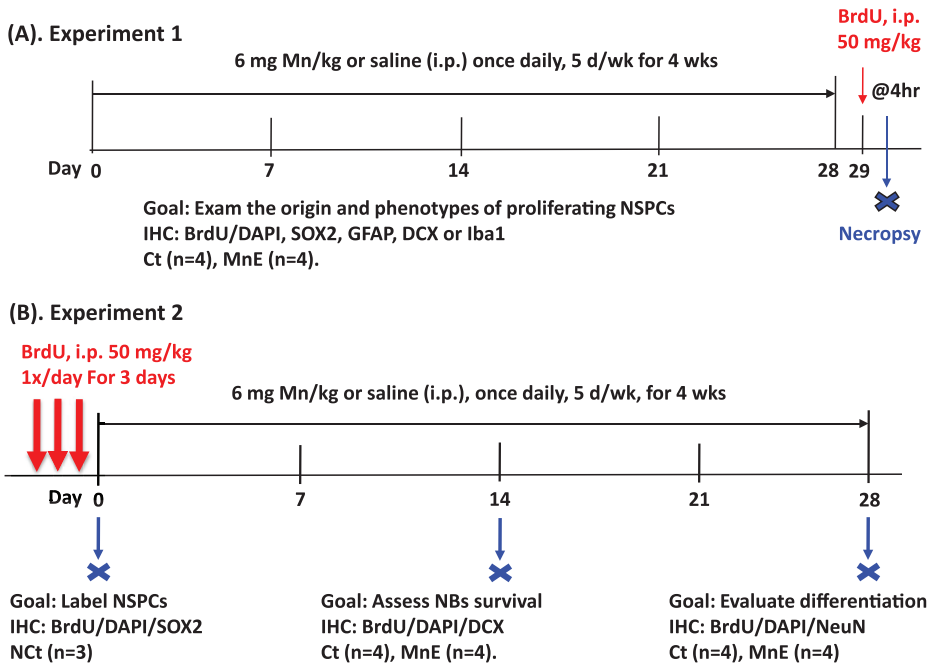


**Figure 1.** Experimental design. A, Experiment 1. Rats received daily IP injections of 6 mg Mn/kg, 5 days/week, for 4 week. Twenty-four hour after the last dose, rats received a single injection of bromodeoxyuridine (BrdU; 50 mg/kg, IP) and were sacrificed 4 h later ($n = 4$/group). B, Experiment 2. BrdU (50 mg/kg, IP) was administered once daily for 3 consecutive days prior to Mn exposure. One group of rats ($n = 3$) was sacrificed 24 h after the last BrdU injection to obtain the initial population of proliferating cells. Two groups of rats, one for control (Ct) and the other for Mn-exposed (MnE) ($n = 4$/each group), received daily IP injections of 6 mg Mn/kg or saline for 14 days. They were sacrificed 24 h later. Another two groups of rats (Control and Mn-Exposed, $n = 4$/group) received daily Mn and saline injections, respectively, for 28 days and were sacrificed 24 h after the last dose.

Mn exposure disrupted the survival and differentiation of NSPCs in the HDG. Rats received IP injection of BrdU at 50 mg/kg once daily for 3 consecutive days to label the total population of newborn progenitors in adult HDG prior to the first Mn dose. Animals were necropsied on day 0, day 14, and day 28 after Mn exposure (Figure 1B).

*Tissue preparation*. All animals were anesthetized using ketamine/xylazine (75:10 mg/kg, 1 mg/kg IP), and perfused transcardially with ice-cold saline followed by 4% PFA in phosphate-buffered saline (PBS). Brains were then removed from the skull and postfixed in 4% PFA for 24 h, followed by dehydration process in 30% sucrose for 7 days. Serial 30-μm thick coronal or sagittal sections were cut using a microtome and stored in cryoprotectant solution at –20°C. Specifically, for coronal and sagittal sectioning, the brains were sectioned roughly from Bregma 2.0 to –6.0 mm (coronal) and Lateral 0.2 to 4.0 mm/hemisphere (sagittal) according to the rat brain atlas in order to cover the entire distance of the hippocampus, which yielded about 250–270 sections/brain (coronal) and 125–135 sections/hemisphere (sagittal). All of the coronal sections were placed in a 12-well plate in serial order, and all of the sagittal sections collected from one hemisphere were placed in 6 wells of the 12-well plate in serial order. Each well contains about 18–22 sections for both coronal and sagittal sections, which accounts for 1/12 of the total brain sections. The 18–22 sections within the same well and with the same well number order across all animals were then processed for immunohistochemical analysis.

*Immunohistochemistry staining*. Series of every 12th section (360 μm interval), covering the distance of the lateral ventricle, were processed for immunohistochemistry (IHC) analysis. Free-floating sections were washed with PBS (3 × 10 min/wash), incubated in 2 N HCl for 2 h at room temperature (RT), and then blocked in 0.1 M borate buffer for 15 min (pH 8.4). After 3 washes with PBS (10 min/wash), sections were incubated in blocking solution (0.3% Triton X-100, 1% BSA, and 5% normal goat serum in PBS) for 1.5 h at RT, followed by overnight incubation with primary antibodies at 4°C. The sections were washed with PBS (3× 10 min) and incubated with secondary antibodies for 2 h at RT. After incubation with 4′,6-diamidino-2-phenylindole (DAPI) for 15 min at RT, sections were rinsed with PBS (3× 10 min) and mounted using Fluorescent Mount G.

The procedure to combine the IHC staining with various primary antibodies was as followed: (1) to examine the proliferation of newly-born progenitor cells, brain sections were stained with mouse anti-BrdU (1:500) and rabbit anti-GFAP primary antibodies (1:1000), followed by incubation with Alexa Fluor 555 goat anti-mouse IgG (H + L) antibody (1:500) and Alexa Fluor 488 goat anti-rabbit IgG (H + L) antibody (1:1000); (2) to identify whether the BrdU(+) cells were DCX(+) neuroblasts, brain sections were labeled with mouse anti-BrdU primary antibody (1:500) and rabbit anti-DCX primary antibodies (1:1000), followed by treatment with Alexa Fluor 555 goat anti-mouse IgG (H + L) antibody (1:500) and Alexa Fluor 488 goat anti-rabbit IgG (H + L) antibody (1:1000); and (3) to verify whether BrdU(+) cells were further differentiated into interneurons being integrated into the OB circuitry, brain sections were incubated with mouse anti-BrdU primary antibody (1:500) and rabbit anti-NeuN primary antibodies (1:1000), followed by incubation with Alexa Fluor 555 goat anti-mouse IgG (H + L) antibody (1:500) and Alexa Fluor 488 goat anti-rabbit IgG (H + L) antibody (1:1000).

*Microscopy and imaging processing*. After IHC processing, brain sections were examined using a Nikon TE2000-U inverted microscope equipped with a Nikon A1 confocal system (Nikon Instruments, Melville, NY). Images were taken using the software NIS Elements AR (v4.20). All images were reassembled and labeled in Photoshop CC.

For cell counting, all sections were analyzed with appropriate filter or laser combinations under an objective lens of 20×/0.75 (DIC N2, ∞0.17 WD). Large image plus Z-Stack scanning was employed to confine the entire HDG from either coronal or sagittal sections. Z-Stacking images with higher magnifications were captured under the objective lens of 60×/1.49 oil (DIC N2, ∞0.13–0.21) in order to verify the colocalizations of different cellular markers.

*Cell counting*. IHC was performed simultaneously on sections from different groups to detect the target cells. Series of every 12th section (30 μm thickness, 360 μm apart) through each lateral ventricle were processed. The cell density was determined through a blinded quantitative histological analysis. A profile count method was used. Every single BrdU(+) cells (including partial of BrdU(+) nuclei at the border of section), or BrdU and specific cell marker (GFAP for astrocytes, DCX for neuroblasts, NeuN for mature neurons, and Iba1 for microglial cells) double-labeled cells in the different subregion of HDG in the multiplanes throughout the entire 30 μm section, were counted under the fluorescent or confocal microscope using the large Z-stacking images through the entire series of sections.

The double-labeled cells were determined as follows. BrdU was used as an indicator. When the BrdU(+) cell was identified, the channel was switched to those matching the cell-specific markers. Those double-labeled cells were considered the target cells for cell counting. The total number of quantified cells was justified by correction (Coggeshall and Lekan, 1996). The total number of BrdU(+) or double-labeled cells were then calculated by the equation [the total cell number = (the sum of actual cell counting number) × 12], and expressed as total number/target region/brain ($n = 3$ or 4 brains for each group).

*Statistical analyses*. All data are presented as mean ± SD. Statistical analyses of the differences between control and Mn-exposed groups were carried out by a Student's *t*-test. Comparisons of differences among the negative control baseline group (day 0), the control and Mn-exposed groups within the 2- and 4-week time points were analyzed by one-way ANOVA with post hoc comparisons by the Dunnett's test. Comparisons of differences between control and Mn-exposed groups within the 2- and 4-week time points were analyzed by 2-way ANOVA with post hoc comparisons by the Tukey test. All the statistical analyses were conducted using IBM SPSS for Windows (version 22.0). The differences between two means were considered significant for $p \leq .05$.

## RESULTS

### *Experiment 1: NSPC Proliferation in the Adult HDG Following Subchronic Mn Exposure*

*Subchronic Mn exposure reduces the proliferation of NSPCs in the adult HDG*. The experimental designed in Figure 1A allowed us to assess the newly proliferated NSPCs in the adult HDG within a 4-h time window after 4-week subchronic Mn exposure. In the saline control group, the newly proliferating cells (total number: $5.97 \pm 0.81 \times 10^3$) that were labeled by the BrdU were generally scattering in the HDG; yet a remarkable proportion of these BrdU(+) cells were distributed within a narrow zone between the GCL and the hilus of the HDG where the SGZ is located (Figure 2A). After 4-week Mn exposure, the numbers of BrdU(+) cells in the HDG subregions of SGZ ($1.39 \pm 0.26 \times 10^3$), hilus ($1.15 \pm 0.10 \times 10^3$), and molecular layer (ML) ($1.21 \pm 0.27 \times 10^3$) (Figure 2B) were significantly reduced, as compared with those of the saline control (SGZ: $2.37 \pm 0.47 \times 10^3$; hilus: $1.65 \pm 0.26 \times 10^3$; and ML: $1.90 \pm 0.22 \times 10^3$) ($p < .05$, Figure 2C). The data suggested that subchronic Mn exposure suppressed cell proliferation in the adult HDG, which is opposite to our previous findings in the adult subventricular zone (SVZ) where Mn promotes the proliferation of NSPCs in that region (Fu *et al.*, 2015a, 2016), indicating that Mn exposure has a differential effect in these two primary neurogenic niches in the adult brain.

Within the 4-h time frame, the proliferating NSPCs expressing the cellular marker Sox2 in the SGZ were colabeled with BrdU (Figs. 2A and 2B). By identifying Sox2/BrdU/DAPI(+) cells, most of the BrdU and Sox2 colabeled cells were found within the control SGZ with a few located in the hilus and ML (Figure 2A). BrdU and Sox2 double positive cell numbers were significantly decreased in the SGZ and hilus, following subchronic Mn exposure (Figs. 2B and 2D). These findings indicated that the majority of the newly proliferating cells were Sox2(+) NSPCs within the adult SGZ region and the proliferation of these adult born NSPCs were significantly inhibited by subchronic Mn exposure.

Comparing the distribution patterns of newly proliferating BrdU(+) cells in different subregions of the adult HDG indicated that the control SGZ harbored the most proliferating cells (40%), followed by the ML (32%), hilus (27%), and GCL (1%) (Figure 2E). Similarly in the Mn-exposed adult HDG, most of the newborn cells were distributed in the SGZ (37%), followed by the ML (32%), hilus (30%), and GCL (1%) (Figure 2F). Although the counted cell numbers in these subregions were significantly higher in controls than the Mn-exposed group (Figs. 2C–F), subchronic Mn exposure did not seem to change the distribution pattern (%) within these regions, suggesting that Mn may suppress the general proliferation throughout different regions of the adult HDG.

*Phenotypical analyses of newly proliferating cells in Mn-exposed adult rat HDG*. The proliferation phase is the initial phase of hippocampal adult neurogenesis (Kempermann *et al.*, 2015). Adult-born neurons originated from the type 1 radial glia-like precursor cells located in the narrow SGZ are quiescent neural cells expressing the cytoskeletal marker GFAP and the transcription factor Sox2 (Encinas *et al.*, 2006; Kempermann *et al.*, 2015). Upon activation, type 1 quiescent progenitors can quickly develop into transiently amplifying types 2a and 2b precursor cells (Von Bohlen Und Halbach, 2007): type 2a cells express Sox2 and may or may not express GFAP, whereas type 2b precursors do not express Sox2 but express the immature neuronal marker DCX (Kempermann *et al.*, 2015). These precursor cells then begin to appear the characteristics of type 3 neuroblasts that express DCX (Kempermann *et al.*, 2015). A proportion of the neuroblasts undergoes the differentiation and becomes mature neurons that express the mature neuronal marker NeuN (Espósito *et al.*, 2005). BrdU labels all the proliferating cell types, but does not distinguish one from another. The current study used the triple-staining technique to identify the cell types by colocalizing the BrdU-labeled nuclei with the nuclei marker DAPI and other cellular markers (GFAP, Sox2, DCX, and Iba1) in the HDG. Under the high magnification, the BrdU-labeled newborn cells

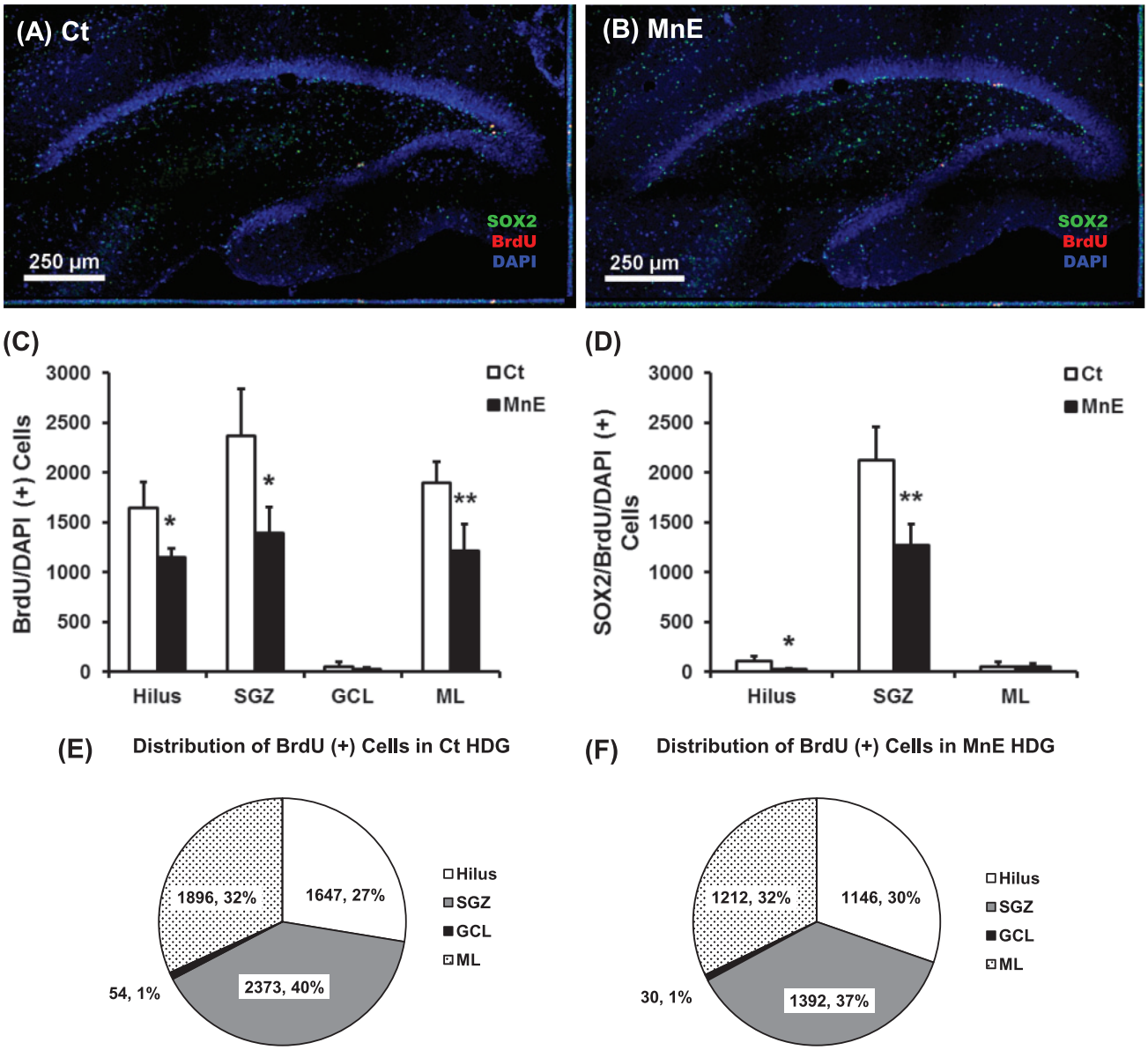


**Figure 2.** Cell proliferation in adult hippocampal dentate gyrus (HDG) with or without subchronic Mn exposure. A, Adult rats received saline as the control (Ct). B, Rats received Mn injections as the Mn-exposed group (MnE). See Figure 1A for detailed experimental design. Newborn cells were labeled with BrdU (red). 4′,6-Diamidino-2-phenylindole (DAPI) (blue) was used to stain nuclei and delineate the structure of the HDG. C, Quantification of BrdU/DAPI-labeled cells in the HDG subregions (ie, hilus, subgranular zone [SGZ], granule cell layer [GCL], and molecular layer [ML]) of both hemispheres following in vivo subchronic Mn exposure. D, Quantification of Sox2/BrdU/DAPI(+) cells in the HDG of both hemispheres following subchronic Mn exposure. Data represent mean ± SD, $n = 4$. $^{*}p < .05$, as compared with controls. E, Percentage distribution of BrdU-labeled in the control HDG subregions. F, Percentage distribution of BrdU-labeled in the Mn-exposed HDG subregions.

were identified morphologically by their round or oval shape with the size of about 10 μm in diameter, and these cells appeared as small clusters (about 2–6 cells/cluster) along the innermost layer of the GCL where the SGZ resides (Figs. 3A–D). Our Z-stack confocal images of GFAP/BrdU/DAPI triple-staining showed that the BrdU-labeled nuclei were double-labeled with the nuclei marker DAPI in blue color but not associated with the green GFAP signals (Figure 3A: c and d). The observation suggested that these newborn cells were not the radial glial-like GFAP(+) type 1 quiescent progenitor cells. However, when costained with the Sox2 antibody, the red BrdU fluorescent signals were nicely overlapped with the blue DAPI signals and the green Sox2 signals (Figure 3B: b and c), indicating that these newborn cells were the actively proliferating type 2a progenitors. Interestingly, in the DCX/BrdU/DAPI triple-staining, we also observed that some BrdU/DAPI(+) nuclei were surrounded by the green DCX fluorescent and had very short projections (Figure 3C: b and c), suggesting that some of the newborn cells had become the type 2b progenitors and even begun to differentiate into type 3 immature neurons.

Mn exposure has been suggested to cause microglial activation via various inflammatory pathways (Abe *et al.*, 2015; Verina *et al.*, 2011; Zhao *et al.*, 2009). Our previous study has confirmed that Mn exposure increases the number of newly born microglial cells in the adult SVZ; however, this increase is mild but not substantial so that it does not contribute significantly to the overall cell proliferation in the SVZ under Mn influence (Fu *et al.*, 2015a). To investigate whether Mn exposure also induced

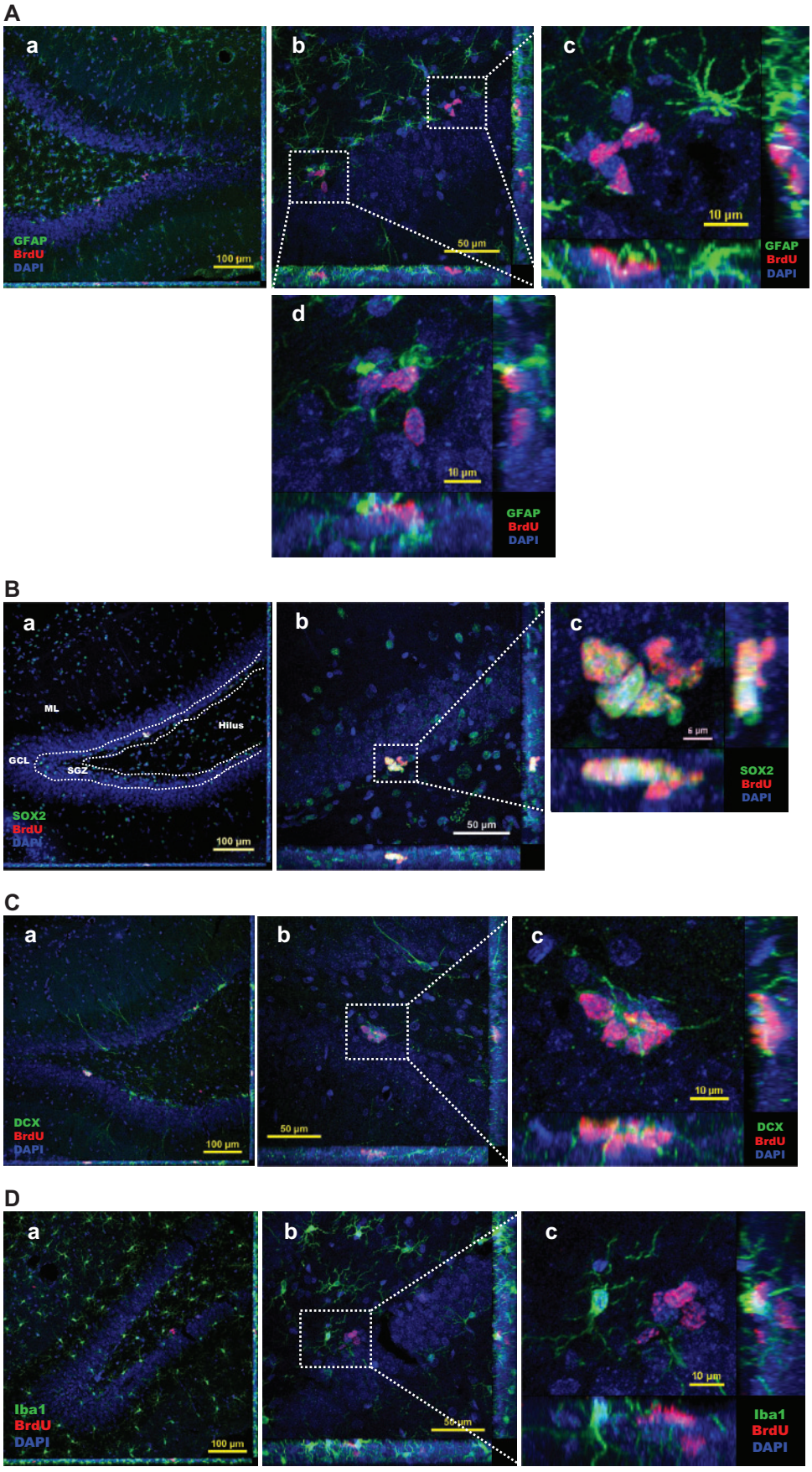


**Figure 3.** Identification of BrdU-labeled proliferating cells in Mn-exposed HDG. A, Triple-staining with GFAP/BrdU/DAPI in Mn-exposed HDG. Two representative images in A-c and A-d show zoom-in Z-stack images with all three merged channels (blue: DAPI; red: BrdU; green: GFAP). B, Colocalization of BrdU with Sox2(+) progenitor

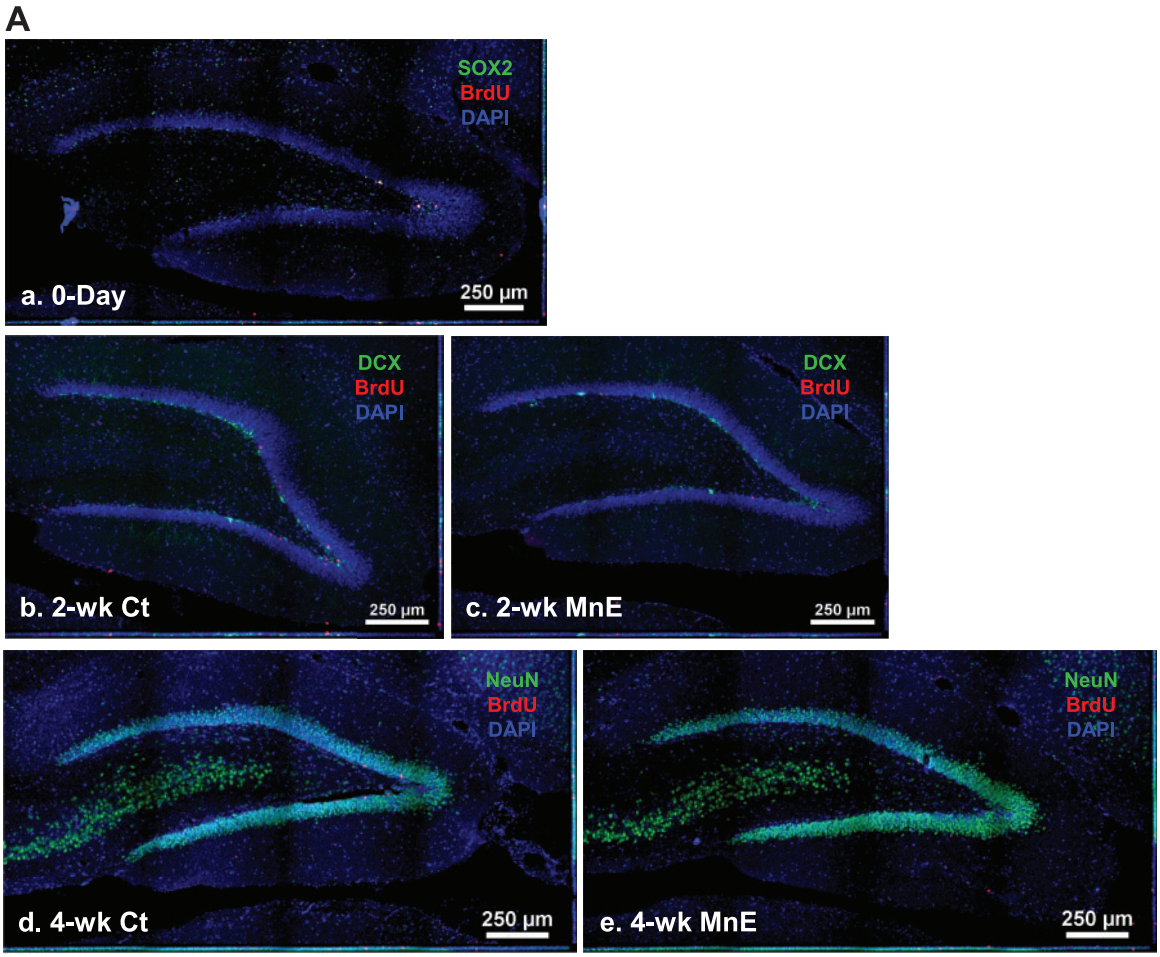


**Figure 4.** Spatial distribution of BrdU-labeled proliferating cells in the adult HDG with or without subchronic Mn exposure. See Figure 1B for detailed experimental design. Sections were triple-labeled with Sox2/BrdU/DAPI (day 0), DCX/BrdU/DAPI (2 weeks), and NeuN/BrdU/DAPI (4 weeks). A, Control brain section prepared after 3-day BrdU injections and at day 0 prior Mn treatment. Image a shows the triple immunostaining of Sox2/BrdU/DAPI (day 0) to identify newly proliferating progenitors in the HDG; images b and c show the triple immunostaining of DCX/BrdU/DAPI to identify immature neurons in the 2-week control and Mn-exposed HDG, respectively; confocal images d and e show the triple immunostaining of NeuN/BrdU/DAPI to identify newborn mature neurons in the 4-week control and Mn-exposed HDG. B, Representative confocal images with Z-stack to show the colocalization of BrdU/DAPI with different cellular markers to distinguish the Sox2(+) newly proliferating progenitors at day 0 HDG (a), DCX(+) immature neurons at 2-week control (b) and Mn-exposed HDG (c), and NeuN(+) mature neurons at 4-week control (d) and Mn-exposed HDG (e). B-a, Negative control brain section prior to Mn exposure. Three-dimensional reconstructions of images a1 and a7 are the zoomed-in images from image B-a to show Sox2/BrdU/DAPI triple-labeled newborn progenitors in the SGZ layer. Images in a2-4 and a8-10 show the red (BrdU), green (Sox2), and blue (DAPI) channels, respectively. Images in a5 and a11 show the merged DAPI/BrdU signals, and images a6 and a12 show the merged BrdU/Sox2 signals. B-b, Control brain section with 2-week saline treatment. The Z-stack confocal image b1 is the zoomed-in image from image B-b to show the colocalization of DCX/BrdU/DAPI(+) immature neurons in the HDG. Images in b2-4 show the red (BrdU), green (DCX), and blue (DAPI) channels, respectively. Images in b5 and b6 show the merged DAPI/BrdU, and BrdU/DCX signals, respectively. B-c, Mn-exposed brain section following 2-week Mn exposure. In the zoomed-in HDG (c1), BrdU signals (red) were overlapped with DCX (green). Images in c2-4 show the red (BrdU), green (DCX), and blue (DAPI) channels, respectively. Images in c5 and c6 show the merged DAPI/BrdU, and BrdU/DCX signals, respectively. B-d, Control brain section with 4-week saline treatment. The Z-stack images in d1 and d7 are zoomed-in images from image B-d to show the colocalization of NeuN/BrdU/DAPI(+) mature neurons in the HDG. Images in d2-4 and d8-10 show the red (BrdU), green (NeuN), and blue (DAPI) channels, respectively. Images in d5-6 and d11-12 show the merged DAPI/BrdU, and BrdU/NeuN signals, respectively. B-e, Mn-exposed brain section following 4-week Mn exposure. In the zoomed-in HDG (e1), BrdU signals (red) were overlapped with NeuN (green). Images in e2-4 show the red (BrdU), green (NeuN), and blue (DAPI) channels, respectively. Images in e5 and e6 show the merged DAPI/BrdU, and BrdU/NeuN signals, respectively.

microglia in the adult HDG, we performed the triple-staining of BrdU/DAPI with the Iba1, a well-known marker for microglia. A representative confocal image with Z-stack projection in Figure 3D suggested that Iba1 signals were not associated with BrdU signals, suggesting that Mn exposure did not activate microglia in the HDG.

### *Experiment 2: Survival and Differentiation of Newborn NSPCs in the HDG Following Subchronic Mn Exposure*

*Time-dependent reduction of newborn cells in the adult HDG, and effect of Mn exposure.* To evaluate the effects of subchronic Mn exposure on the entire process of adult hippocampal neurogenesis, we labeled most of the newly adult-born cell populations in the

**Figure 3.** Continued

cells. Sections were triple-stained with Sox2/BrdU/DAPI in Mn-exposed HDG. A representative image in B-c shows a zoom-in Z-stack image with all three merged channels (blue: DAPI; red: BrdU; green: Nestin). C, Colocalization of BrdU with DCX(+) immature neurons. Sections were triple-stained with DCX/BrdU/DAPI in Mn-exposed HDG. A representative image in C-c shows a zoom-in Z-stack image with all three merged channels (blue: DAPI; red: BrdU; green: DCX). D, Triple-staining with Iba1/BrdU/DAPI in Mn-exposed HDG. A representative image in D-c shows a zoom-in Z-stack image with all three merged channels (blue: DAPI; red: BrdU; green: Iba1).

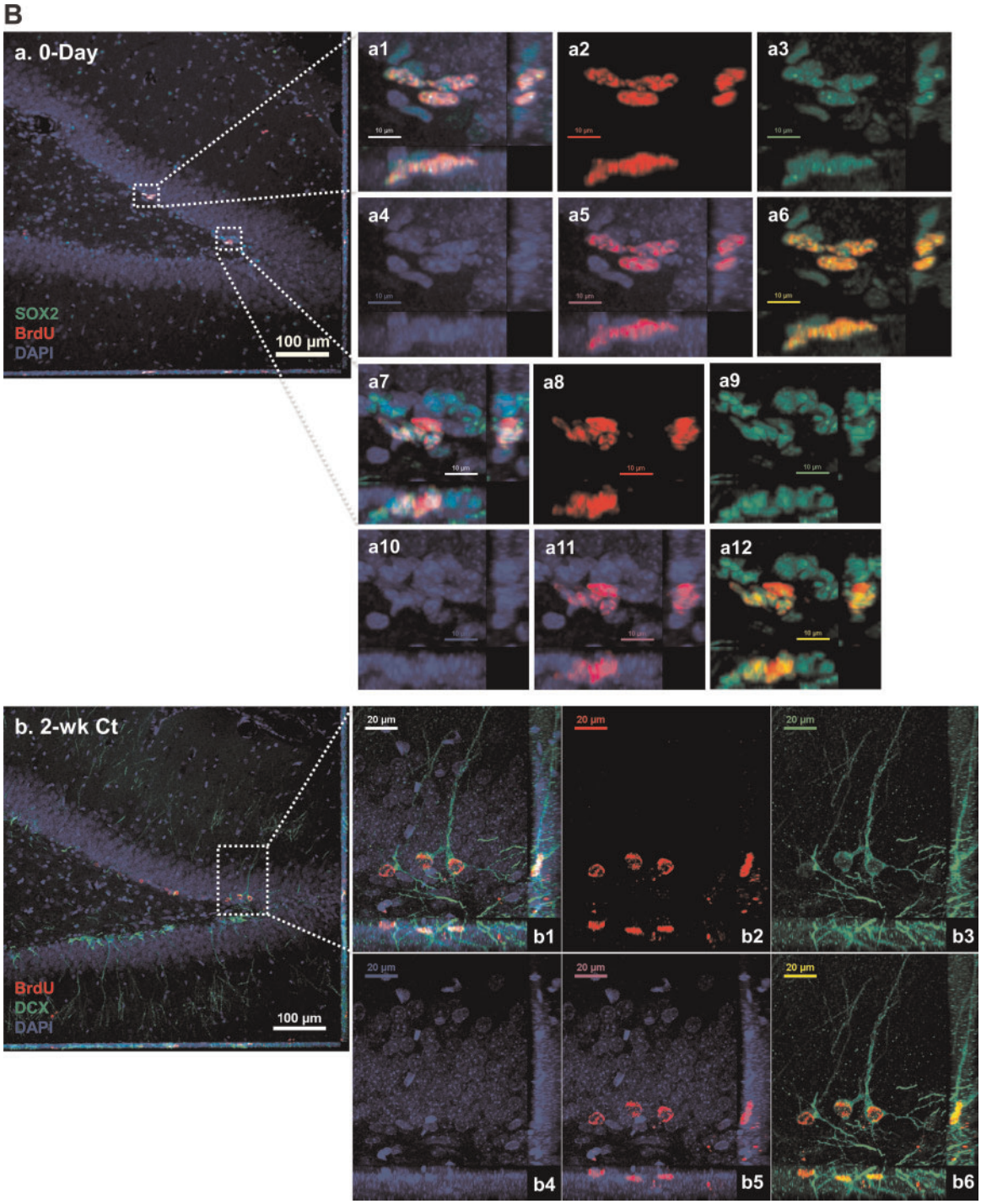


**Figure 4.** (continued).

HDG with BrdU (50 mg/kg, IP, once daily for 3 continuous days) prior to Mn exposure and then traced these newborn progenitors on day 0, 2-week, and 4-week after Mn exposure, and investigated their survival and differentiation in the HDG (Figure 1B).

After BrdU administration for 3 days (on Day 0 without Mn exposure), the cell counting data showed a total population of $9.81 \pm 0.55 \times 10^3$ BrdU(+) newborn proliferating cells in the HDG; these cells were primarily distributed in the SGZ ($4.85 \pm 0.42 \times 10^3$), followed by the hilus ($2.77 \pm 0.22 \times 10^3$), ML ($2.01 \pm 0.34 \times 10^3$) and GCL ($0.18 \pm 0.10 \times 10^3$) (Figs. 4A-a and 5A and 5B). By counting the triple-staining cells with Sox2/BrdU/DAPI (Figs. 4A-a and 4B-a), it was clear that most of the proliferating cells were Sox2(+) progenitors ($4.28 \pm 0.57 \times 10^3$) within the SGZ at the day 0 (Figure 5C), suggesting an active amplification during the 3-day BrdU administration prior to Mn exposure.

At 2-week after saline treatment in the control group, our Z-stack confocal images showed that the BrdU-labeled newborn cells had developed into the DCX(+) immature neuron with the

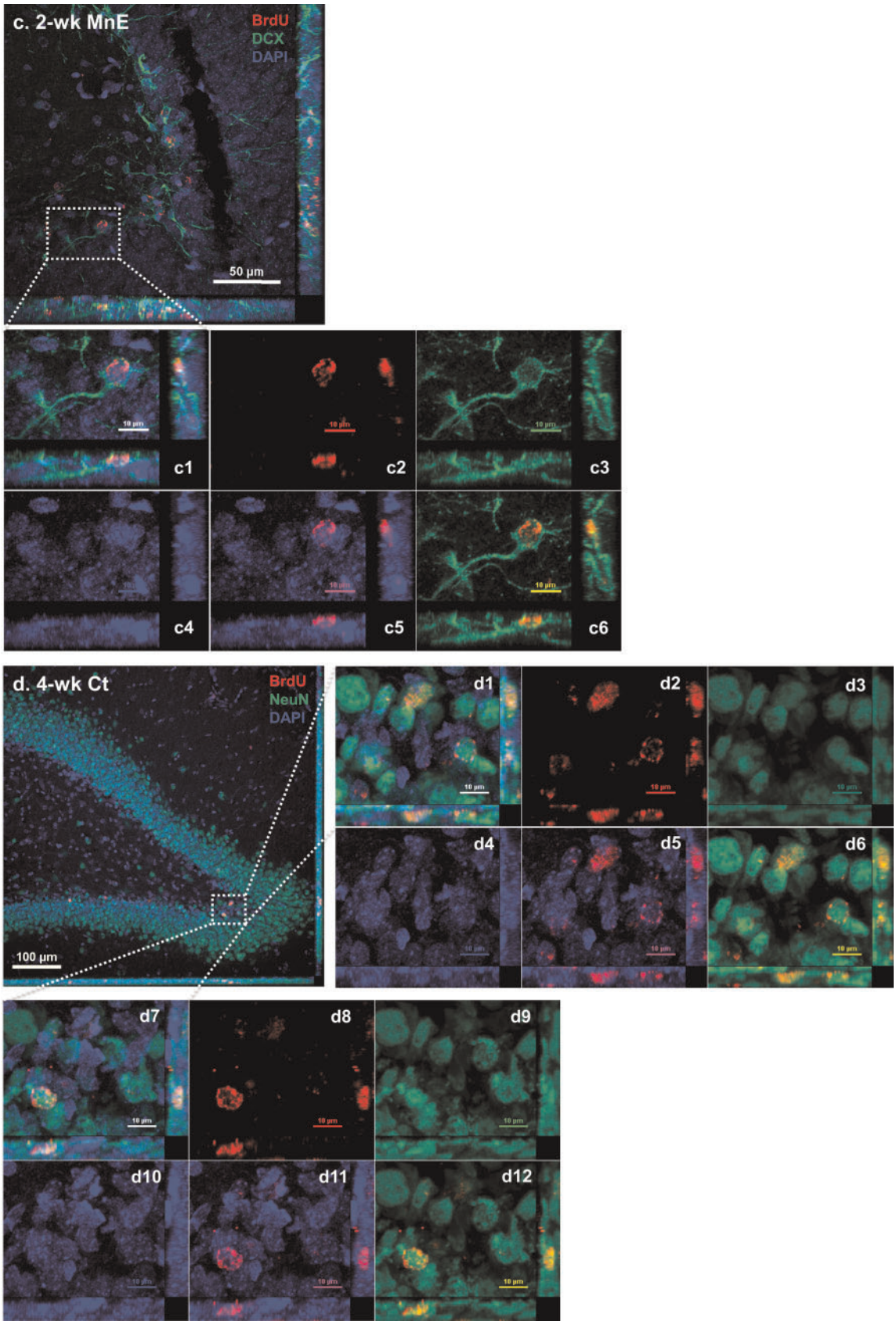


Figure 4. (continued).

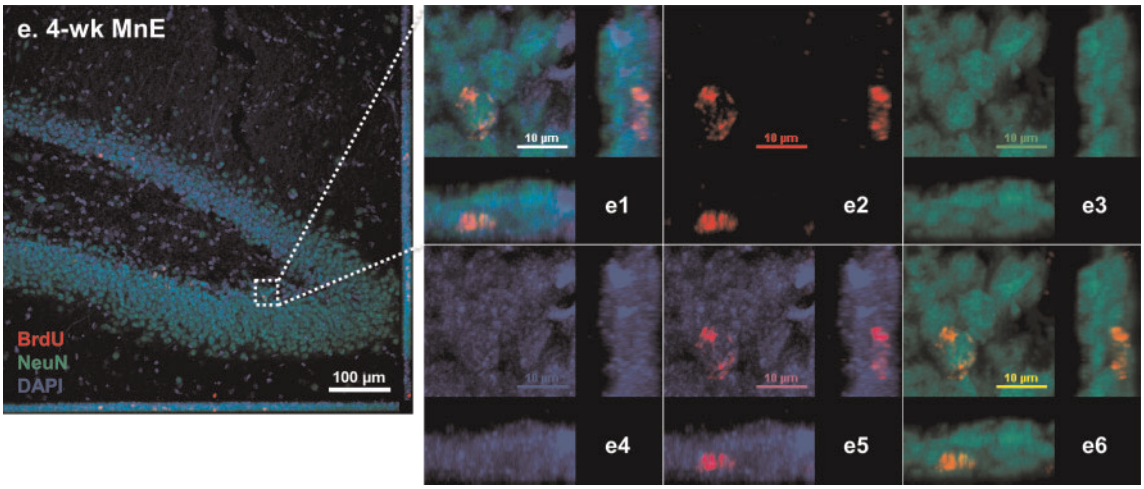


**Figure 4.** (continued).

cell bodies migrating into the GCL, the long extended projections extruding toward the ML, and the dendritic branches protruding into the outer ML (Figure 4B-b). In addition, the total BrdU(+) cells in the HDG was reduced to $7.84 \pm 0.51 \times 10^3$, as compared with the day-0 proliferating population, indicating that about 20% of the newborn cells disappeared as a part of their differentiation process during this survival phase (Figs. 5A and 5B). The number became even less in the control HDG at 4-week ($4.78 \pm 0.40 \times 10^3$) (Figs. 5A and 5B). By the end of 4-week, the BrdU prelabeled cells showed the characteristics of mature neurons by expressing the mature neuronal marker NeuN (Figure 4B-d). Significant time-dependent reductions of BrdU(+) newborns cells appeared in the subregions of SGZ, hilus, and ML ($p < .01$), with the exception in the GCL where the BrdU(+) cells were increased (2-week: $1.14 \pm 0.10 \times 10^3$; 4-week: $1.87 \pm 0.18 \times 10^3$) ($p < .01$, Figs. 5A and 5B). This time-dependent increase of proliferating cells in the GCL seemed likely to suggest that the adult NSPCs fulfilled the proliferation, differentiation, and migration from the SGZ toward the GCL prior to their maturation into granule neurons during the 4-week time frame.

In the same time course, the Mn-exposed animal showed similar time-dependent reductions in the total BrdU-labeled newborn cells, as well as in the subregions of SGZ, hilus, and ML ($p < .01$, Figs. 5A and 5B). A significant time-dependent increase was also observed in the HDG subregion of GCL (2-week: $0.68 \pm 0.10 \times 10^3$; 4-week: $1.16 \pm 0.18 \times 10^3$) ($p < .01$, Figs. 5A and 5B). By comparing the cell counting data between the control and Mn-exposed groups, there were statistically significant fewer BrdU(+) cells in Mn exposed HDG than in controls at the same time points and within the same subregions ($p < .01$, Figs. 5A and 5B).

In addition, the Z-stack confocal images of Mn-exposed HDG confirmed the colocalization of BrdU with DCX cells, suggesting that newly proliferating cells had become the immature neurons at 2 weeks post-treatment (Figure 4B-c). However, the newborn DCX(+) immature neurons in the Mn-exposed HDG (Figure 4B-c) appeared to have aberrantly oriented basal dendrite, shorter projections and less dendritic branching, as compared with the controls (Figure 4B-b); the latter observation indicated that Mn exposure may interfere with the normal development of NSPCs into immature neurons by impeding the growths of neuronal projections, dendrites and axons, which eventually led to an impaired adult neurogenesis. Similar to the control (Figure 4B-d), the BrdU prelabeled NSPCs were able to differentiated into NeuN(+) mature neurons at the end of the 4-week Mn exposure (Figure 4B-e).

*Mn exposure significantly reduces the survival and inhibits the differentiation of BrdU(+) cells in the adult HDG.* Our previous data demonstrate a reduction of the surviving adult-born immature neurons and an ensuing inhibition of their differentiation into mature neurons in the OB following subchronic Mn exposure (Fu *et al.*, 2016). To assess whether the same could happen in the SGZ, brain tissues at day 0, 2-week, and 4-week after the Mn exposure were collected and triple-labeled with Sox2/BrdU/DAPI for NSPCs, DCX/BrdU/DAPI for immature neurons, and NeuN/BrdU/DAPI for mature neurons in the HDG subregions of SGZ and GCL. Noticeably, a 2-week time frame is considered as a critical and early survival time for the newborn and immature neurons to survive and differentiate into mature granule neurons (Christian *et al.*, 2014). Our cell counting data revealed a significant time-dependent decrease of triple-labeled cells within the SGZ, and 2-week Mn exposure significantly reduced the DCX/BrdU/DAPI-labeled immature neurons by 39.3% as compared with the control ($p < .01$, Figs. 5C and 5D).

With the time, the DCX/BrdU/DAPI-labeled immature neurons can further differentiate into NeuN/BrdU/DAPI-labeled mature neurons in GCL. Analyses of the triple-labeled cells in both SGZ and GCL of control rats (Figure 5D left panel) indicated a time-dependent decline of differentiated cells in SGZ, which was accompanied with a time-dependent increase of mature neurons in GCL, indicating that the newborn immature neurons managed to migrate in a short distance from the SGZ to the GCL. In Mn-exposed animals, however, there were significantly fewer DCX(+) immature neurons and NeuN(+) mature neurons in the GCL, when compared with the control GCL at the same time point ($p < .01$, Figure 5D right panel). These observations suggested that Mn exposure decreased the survival of the newborn cells and inhibits their differentiation into the mature neurons in the adult HDG.

To study Mn effect on the time-dependent survival rates of newborn cells, we normalized BrdU(+) cell counts by the total labeled proliferating population at day 0. For the control group, about 80% and 51% of the prelabeled BrdU(+) proliferating cells

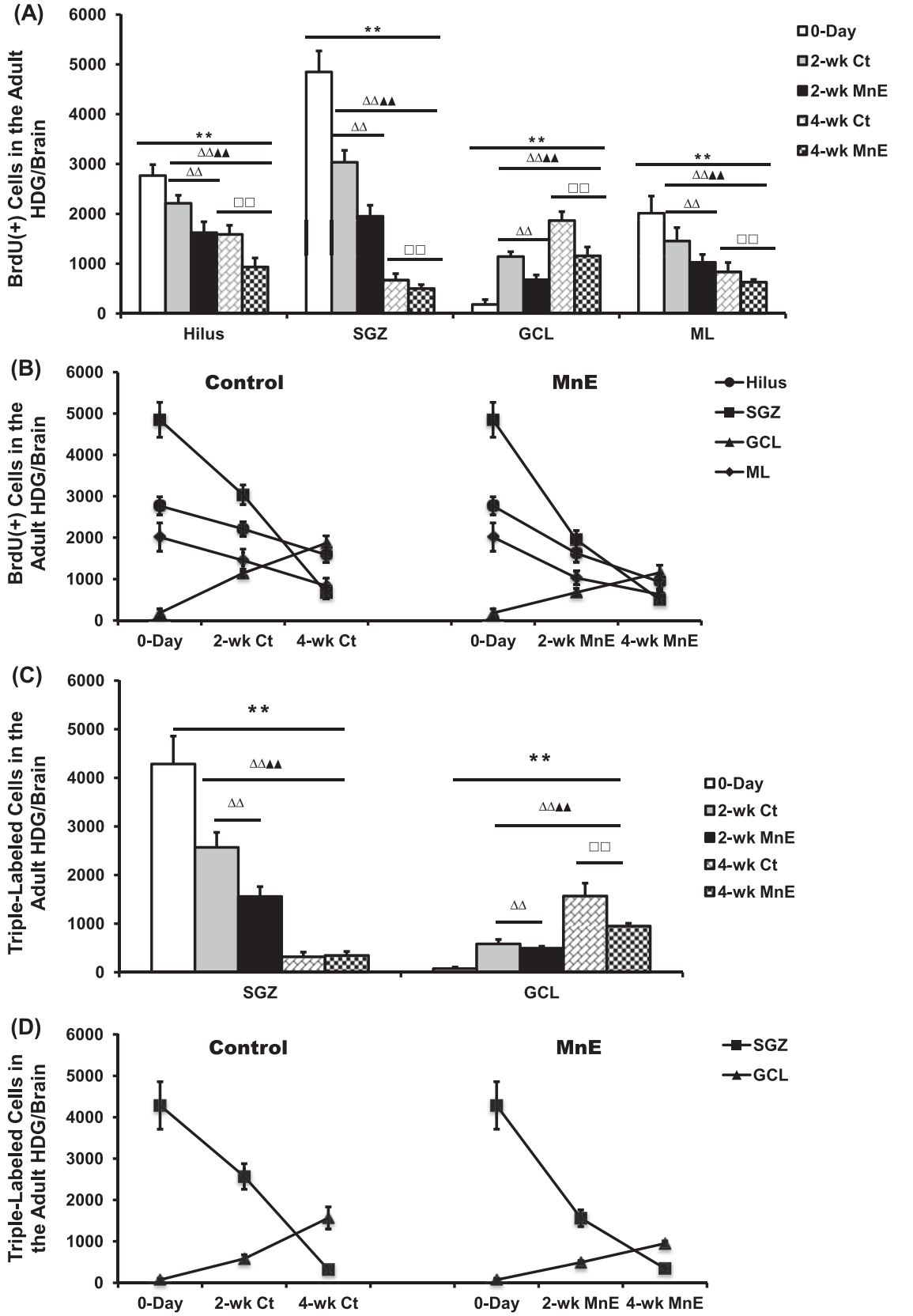


**Figure 5.** Time-dependent reduction of newborn cells in the HDG subregions and effects of Mn exposure. A, Quantification of BrdU(+) cells in the adult HDG subregions of hilus, SGZ, GCL, and ML of all groups. B, Time-dependent changes of BrdU(+) cell counting in the subregions of control and Mn-exposed HDG. C, Quantification of Sox2/BrdU/DAPI (day 0), DCX/BrdU/DAPI (2 weeks), and NeuN/BrdU/DAPI (4 weeks) triple-labeled cells in the adult HDG subregions of SGZ and GCL of all groups. D, Time-dependent changes of triple-labeled cell counting in the SGZ and GCL of control and Mn-exposed HDG. E, Time-dependent survival rates of BrdU-labeled proliferating cells in the entire HDG of all groups. F, Time-dependent survival rates of triple-labeled cells in the entire HDG of all groups. Data represent mean ± SD, $n = 3$–4. $^{**}p < .01$, as compared with the day 0 negative control group; $^{\Delta\Delta}p < .01$, as compared with the 2-week Ct group; $p < .01$, as compared with the 2-week MnE group; $^{\square\square}p < .01$, as compared with the 4-week Ct group.

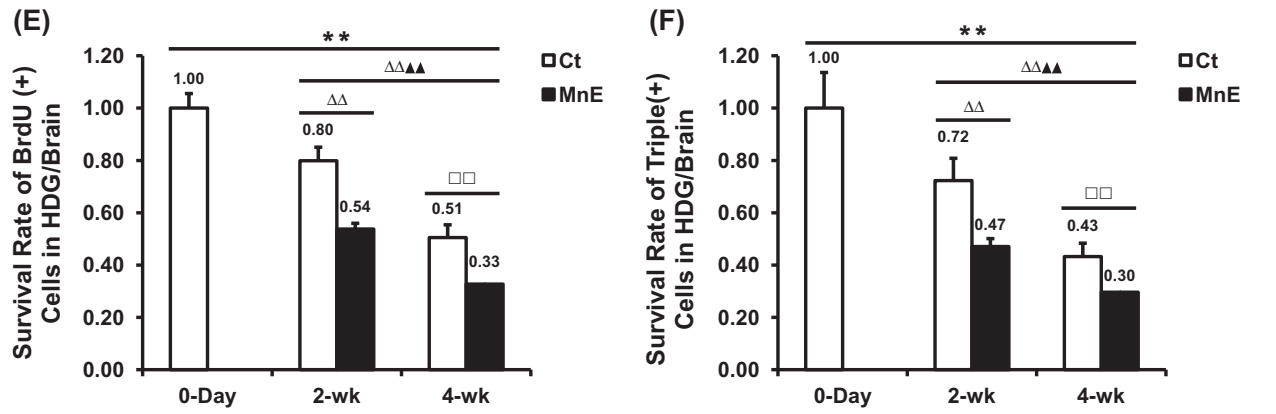


Figure 5. (continued)

survived in the HDG at 2-week and 4-week, respectively (Figure 5E). The survival rates of the newborn cells in Mn-exposed HDG at 2-week and 4-week were 54% and 33%, respectively, which were significantly lower than the corresponding control ($p < .01$, Figure 5E). Data in Figure 5F further showed that in comparison to controls, Mn exposure significantly reduced the survival of DCX/BrdU/DAPI-labeled immature neurons in the HDG at 2 week, and the survival of NeuN/BrdU/DAPI-labeled mature neurons at 4 week ($p < .01$), suggesting an overall suppressed adult neurogenesis in the Mn-exposed HDG.

Although the subchronic Mn exposure induced a profound reduction in the hippocampal adult neurogenesis, there was no significant difference for the HDG subregional distribution between the control and Mn-exposed groups within the same time point (Figure 6A), with the exception of a significant time-dependent migration shift of the newly proliferating cells from the SGZ toward the GCL at the 2-week and 4-week time points (Figure 6B). Collectively, these findings agree with our previous report that in vivo subchronic Mn exposure resulted in an overall decreased adult neurogenesis in the SVZ–RMS–OB system (Fu *et al.*, 2016).

## DISCUSSION

The data from the current study show that subchronic exposure to 6 mg Mn/Kg as $MnCl_2$ for 4 weeks inhibits the proliferation of NSPCs, and the survival and differentiation of newborn cells in the adult HDG. By in-depth analysis of major cell types involving in adult neurogenesis in the SGZ, our immunostaining evidence reveals that the BrdU-labeled proliferating cells affected by Mn toxicity are mainly Sox2(+) type 2a progenitors that primarily located within the SGZ. In addition, when tracing the fate of BrdU-labeled adult-born NSPCs from their initial proliferation to subsequent survival and differentiation in the subregions of HDG, our time-course study demonstrates that *in vivo* subchronic Mn exposure significantly reduces the survival of BrdU(+) adult-born cells and impedes their differentiation into mature neurons in the HDG. However, the distribution pattern of newly proliferating cells throughout the subregions (ie, hilus, SGZ, GCL, and ML) of Mn-exposed HDG remains unchanged, as compared with that of the control. These findings indicate that subchronic Mn exposure impedes the normal adult hippocampal neurogenesis, and a suppressed neural regeneration may damage the neurogenic ability of SGZ to mitigate the neuronal loss caused by Mn-induced neurodegeneration leading to potential physiological consequences such as impaired learning, memory loss and cognitive deficits.

The entire period of adult hippocampal neurogenesis in rodent has been estimated to take about 60 days: (1) 1–7 days for type 1 stem cells to give rise to types 2a and 2b progenitor cells; (2) 8–14 days for type 2 cells to develop into type 3 neuroblasts with depolarized projections toward the ML and the axons toward the CA3 region; (3) 15–30 days for type 3 neuroblasts to differentiate into mature neurons with dendrites and to reach the outer ML and synaptic establishment; and (4) 30–60 days for the mature neurons to fine-tune into fully connected neurons (Aguilar-Arredondo *et al.*, 2015; Christian *et al.*, 2014; Kempermann *et al.*, 2015). In the initial phase, newly proliferating cells originated from the neurogenic niches can be labeled by BrdU, a classic and extensively used marker to study neurogenesis in developing and adult mammalian brain. A single injection of BrdU followed by animal dissection 2–4 h later has been used to identify the origin, proliferation, and phenotypes of newborn cells during S-phase (Lois and Alvarez-Buylla, 1994; Miller and Nowakowski, 1988; Palmer *et al.*, 2000; Taupin, 2007). The current study employed this approach to monitor newly divided BrdU(+) cells for 4 h in the adult HDG following subchronic Mn exposure. Our cell counting data revealed that within this 4-h time frame significantly fewer proliferated cells were labeled by the BrdU in the Mn-exposed HDG than those in the control HDG, suggesting that Mn exposure markedly reduces the proliferation of NSPCs in the adult HDG.

When comparing the distribution of adult born cells in HDG subregions, both control and Mn-exposed groups displayed a similar pattern with the SGZ having a remarkably high proportion of newborn cells, followed by ML and hilus; Mn exposure, however, reduced numbers of newborn cells in the tested subregions. These observations suggest again that Mn exposure inhibits the general proliferation by targeting a wide range of cell populations within the HDG. This wide range effect of Mn on the subpopulations of HDG is consistent with previous study (Kikuchihara *et al.*, 2015). Our findings on the SGZ, however, are deviated from our previous findings where an initial elevated proliferation of NSPCs in the adult SVZ was observed (Fu *et al.*, 2015a, 2016). The discrepancy between the SVZ and HDG implies that Mn may interfere the proliferation of NSPCs through different mechanisms taking into account the cellular compositions, anatomic structures, and biological functions of these two neurogenic niches in the brain.

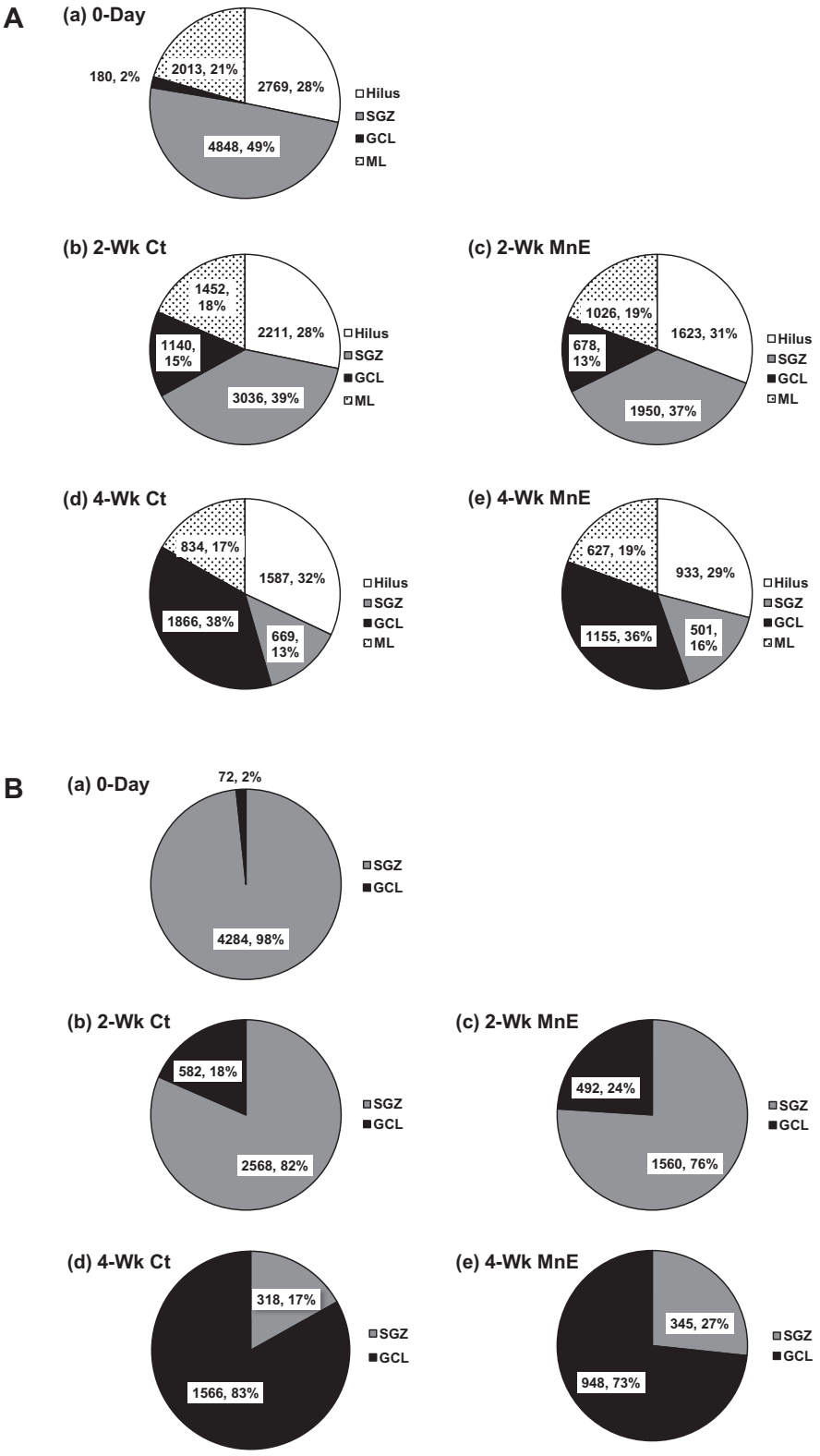


**Figure 6.** Subregional distributions of newborn cells with or without Mn exposure. A, Percentage distributions of BrdU(+) cells in the HDG subregions (ie, hilus, SGZ, GCL, and ML) of all groups. B, Percentage distributions of Sox2/BrdU/DAPI (day 0), DCX/BrdU/DAPI (2 weeks), and NeuN/BrdU/DAPI (4 weeks) triple-labeled newborn cells in the SGZ and GCL of all groups.

Previous findings may provide clues to the Mn-induced reduction of adult neurogenesis in SGZ. First, our previous studies using the same Mn-exposed rat model demonstrate a significantly high amount of Mn in the SVZ, hippocampus, motor cortex, striatum, and choroid plexus (Fu *et al.*, 2014, 2015a,b; Robison *et al.*, 2013; Zheng *et al.*, 2009). Thus, a high amount of Mn accumulated in the SGZ may allow Mn to interact with subcellular targets. Second, at the cellular level, it has been demonstrated that Mn preferentially accumulates in astrocytes and the concentration of Mn can be 50–60 times higher than that in neurons (Aschner *et al.*, 1992; Wedler *et al.*, 1989). Astrocytes play a pivotal role in maintaining normal neuronal functions and regulating neuronal survival, proliferation, differentiation, and neurogenesis in the neurogenic niches (Bak *et al.*, 2006; Blondel *et al.*, 2000; Farina *et al.*, 2007; Liebner *et al.*, 2011). At the subcellular level, the highest Mn concentration in the astrocyte is found within mitochondria (Morello *et al.*, 2008). Thus, exposure of astrocytes to Mn may result in oxidative stress leading to mitochondrial dysfunction and disruption of energy production (Chen and Liao, 2002; Zheng *et al.*, 1998). Recent studies have suggested that the mitochondrial MnSOD is a central molecular player in regulating transitions between quiescent and proliferative growth (Sarsour *et al.*, 2008, 2014), and its activity in brain cells can be inhibited following Mn exposure (Gunter *et al.*, 2006; Ha Mai and Bondy, 2004; Latronico *et al.*, 2013; Parikh *et al.*, 2003; Smith *et al.*, 2017; Szpetnar *et al.*, 2016; Zhang *et al.*, 2004). Considering the fact that the original progenitors in the neurogenic niches are type 1 radial glial-like astrocytic stem cells (which express GFAP), it is reasonable to speculate that the excessive Mn accumulation in the SGZ and hippocampus may disrupt the normal mitochondrial function leading to abnormal proliferation of NSPCs.

Third, our previous data by the XRF with subcellular resolution have demonstrated that copper (Cu) is primarily localized in the GFAP(+) cells in the SVZ (Pushkar *et al.*, 2013), and increased Cu level in the SVZ has been associated with a decreased neurogenesis (Fu *et al.*, 2015b; Pushkar *et al.*, 2013). Further, we also observed an inverse association between Mn and Cu levels in the SVZ (Fu *et al.*, 2015a) and HDG (Robison *et al.*, 2013). Therefore, it is highly possible that the interaction between Mn and Cu within these neurogenic regions may underlie the disturbed proliferation of these astrocytic progenitors. This hypothesis requires further investigation.

Finally, by combing the BrdU labeling with specific cellular markers (ie, GFAP, Sox2, DCX, Iba1, and NeuN), we were able to identify the phenotypes of newborn cells that were affected by Mn exposure during their proliferation, survival, and maturation in the HDG. We observed that the majority of newly proliferated cells were Sox2(+) type 2a precursors distributed primarily in the SGZ, and that Mn exposure markedly reduced the numbers of these precursors. It is therefore possible that Mn may interact with brain-derived neurotrophic factor (BDNF), because BNDF plays a pivotal role in regulating the dendrite development and subsequent structural and functional synaptic plasticity in HDG (Alderson *et al.*, 1990; Cohen-Cory *et al.*, 2010; Horch and Katz, 2002; Gorski *et al.*, 2003; Tolwani *et al.*, 2002; Vigers *et al.*, 2012; Wang *et al.*, 2015). Recent studies in rodents, nonhuman primates, and human workers have also demonstrated a decreased BDNF level in the striatum, hippocampus, and plasma following Mn exposure (Liang *et al.*, 2015; Lv *et al.*, 2014; Stansfield *et al.*, 2014; Sumanont *et al.*, 2007; Zou *et al.*, 2014). Thus, in-depth studies are necessary to further evaluate whether and to what degree Mn exposure may alter the dendritic formation in adult brain and how BDNF may contribute to Mn action. Besides BDNF, Mn has also been reported to reduce expressions of insulin receptor, insulin-like growth factor (IGF-1) receptor, and IGF-II receptor (Tong *et al.*, 2009), indicating that in addition to its direct effect on cell survival and differentiation, Mn may interfere with neurogenesis in the adult HDG by acting on these critical factors.

The current study has several limitations. First, the selected BrdU dose at 50 mg/kg, while sufficient in detecting Mn effect on the entire process of neurogenesis in the adult SGZ as shown in this study, a higher dose of 100–200 mg/kg, which has been used in literatures (Gao *et al.*, 2008, 2011; Gao and Chen, 2011), may allow for labeling more NSPCs in the adult HDG for more accurate estimation of Mn toxicity. Our future studies will adapt the high BrdU dose regimen for SGZ studies. Second, this study was our very first attempt to evaluate the Mn effects on the adult rat hippocampal neurogenesis. Although newly proliferating cells were observed in the subregions of hilus and ML, their identities or phenotypes have not been identified in this study. Further experiments are required to distinguish these cells. Third, we have observed Mn effect on dendrites; but the effects of subchronic Mn exposure on the dendritic length and its entire morphological formation as well as on axons in adult-born neuron in the HDG remain unexamined. In addition, the molecular mechanisms of Mn toxicity on adult neurogenesis have not been investigated in this study. Finally, with regard to Mn toxicity on hippocampal function, it is necessary to investigate the hippocampal function-associated behavioral changes following subchronic Mn exposure.

In conclusion, the data presented in the current study demonstrate that subchronic exposure to Mn leads to reduced cell proliferation, diminished survival of adult-born neurons, and inhibited maturation process in the adult HDG. Our findings are the beginning of our understanding of the relationship between Mn neurotoxicity and adult neurogenesis in the HDG. Future in-depth investigations to explore the underlying mechanisms are strongly recommended.

## FUNDING

Supported in part by NIH/National Institute of Environmental Health Sciences (ES008146 and ES027078 to W.Z. and ES025750 to J.R.C).

## REFERENCES

Abe, H., Ohishi, T., Nakane, F., Shiraki, A., Tanaka, T., Yoshida, T., and Shibutani, M. (2015). Exposure to $MnCl_2{\cdot}4H_2O$ during development induces activation of microglial and perivascular macrophage populations in the hippocampal dentate gyrus of rats. *J. Appl. Toxicol.* **35**, 529–535.

Aguilar-Arredondo, A., Arias, C., and Zepeda, A. (2015). Evaluating the functional state of adult-born neurons in the adult dentate gyrus of the hippocampus: From birth to functional integration. *Rev. Neurosci.* **26**, 269–279.

Akai, F., Maeda, M., Suzuki, K., Inagaki, S., Takagi, H., and Taniguchi, N. (1990). Immunocytochemical localization of manganese superoxide-dismutase (Mn-SOD) in the hippocampus of the rat. *Neurosci. Lett.* **115**, 19–23.

Alderson, R. F., Alterman, A. L., Barde, Y. A., and Lindsay, R. M. (1990). Brain-derived neurotrophic factor increases survival and differentiated functions of rat septal cholinergic neurons in culture. *Neuron* **5**, 297–306.

Aschner, J. L., and Aschner, M. (2005). Nutritional aspects of manganese homeostasis. *Mol. Aspects Med.* **26**, 353–362.

Aschner, M., Gannon, M., and Kimelberg, H.K. (1992). Manganese uptake and efflux in cultured rat astrocytes. *J Neurochem* **58**(2), 730–735.

Aschner, M., Guilarte, T. R., Schneider, J. S., and Zheng, W. (2007). Manganese: Recent advances in understanding its transport and neurotoxicity. *Toxicol. Appl. Pharmacol.* **221**, 131–147.

Bak, L. K., Schousboe, A., and Waagepetersen, H. S. (2006). The glutamate/GABA-glutamine cycle: Aspects of transport, neurotransmitter homeostasis and ammonia transfer. *J. Neurochem.* **98**, 641–653.

Barbeau, A., Inoué, N., and Cloutier, T. (1976). Role of manganese in dystonia. *Adv. Neurol.* **14**, 339–352.

Blecharz-Klin, K., Piechal, A., Joniec-Maciejak, I., Pyrzanowska, J., and Widy-Tyszkiewicz, E. (2012). Effect of intranasal manganese administration on neurotransmission and spatial learning in rats. *Toxicol. Appl. Pharmacol.* **265**, 1.

Blondel, O., Collin, C., McCarran, W. J., Zhu, S., Zamostiano, R., Gozes, I., Brenneman, D. E., and McKay, R. D. (2000). A glia-derived signal regulating neuronal differentiation. *J. Neurosci.* **20**, 8012–8020.

Bowler, R. M., Gysens, S., Diamond, E., Booty, A., Hartney, C., and Roels, H. A. (2003). Neuropsychological sequelae of exposure to welding fumes in a group of occupationally exposed men. *Int. J. Hyg. Environ. Health* **206**, 517–529.

Bowler, R. M., Gysens, S., Diamond, E., Nakagawa, S., Drezgic, M., and Roels, H. A. (2006). Manganese exposure: Neuropsychological and neurological symptoms and effects in welders. *Neurotoxicology* **27**, 315–326.

Carvalho, C. F., Menezes-Filho, J. A., de Matos, V. P., Bessa, J. R., Coelho-Santos, J., Viana, G. F., Argollo, N., and Abreu, N. (2014). Elevated airborne manganese and low executive function in school-aged children in Brazil. *Neurotoxicology* **45**, 301.

Chen, C. J., and Liao, S. L. (2002). Oxidative stress involves in astrocytic alterations induced by manganese. *Exp. Neurol.* **175**, 216–225.

Christian, K. M., Song, H., and Ming, G. L. (2014). Functions and dysfunctions of adult hippocampal neurogenesis. *Annu. Rev. Neurosci.* **37**, 243–262.

Clark, R. E., Zola, S. M., and Squire, L. R. (2000). Impaired recognition memory in rats after damage to the hippocampus. *J. Neurosci. Off. J. Soc. Neurosci.* **20**, 8853.

Coggeshall, R. E., and Lekan, H. A. (1996). Methods for determining numbers of cells and synapses: A case for more uniform standards of review. *J. Comp. Neurol.* **364**, 6–15.

Cohen-Cory, S., Kidane, A. H., Shirkey, N. J., and Marshak, S. (2010). Brain-derived neurotrophic factor and the development of structural neuronal connectivity. *Dev. Neurobiol.* **70**, 271–288.

Crossgrove, J. S., and Zheng, W. (2004). Manganese toxicity upon overexposure. *NMR Biomed.* **17**, 544–553.

Dietz, M. C., Ihrig, A., Wrazidlo, W., Bader, M., Jansen, O., and Triebig, G. (2001). Results of magnetic resonance imaging in long-term manganese dioxide-exposed workers. *Environ. Res.* **85**, 37–40.

Dydak, U., Jiang, Y. M., Long, L. L., Zhu, H., Chen, J. A., Li, W. M., Edden, R. A. E., Hu, S. G., Fu, X., Long, Z. Y., *et al.* (2011). In vivo measurement of brain GABA concentrations by magnetic resonance spectroscopy in smelters occupationally exposed to manganese. *Environ. Health Perspect.* **119**, 219–224.

Eichenbaum, H. (2004). Hippocampus: Cognitive processes and neural representations that underlie declarative memory. *Neuron* **44**, 109e120.

Encinas, J. M., Vaahtokari, A., and Enikolopov, G. (2006). Fluoxetine targets early progenitor cells in the adult brain. *Proc. Natl. Acad. Sci. U.S.A.* **103**, 8233–8238.

Espósito, M. S., Piatti, V. C., Laplagne, D. A., Morgenstern, N. A., Ferrari, C. C., Pitossi, F. J., and Schinder, A. F. (2005). Neuronal differentiation in the adult hippocampus recapitulates embryonic development. *J. Neurosci.* **25**, 10074–10086.

Farina, C., Aloisi, F., and Meinl, E. (2007). Astrocytes are active players in cerebral innate immunity. *Trends Immunol.* **28**, 138–145.

Fitsanakis, V. A., Thompson, K. N., Deery, S. E., Milatovic, D., Shihabi, Z. K., Erikson, K. M., Brown, R. W., and Aschner, M. (2009). A chronic iron-deficient/high manganese diet in rodents results in increased brain oxidative stress and behavioral deficits in the morris water maze. *Neurotox. Res.* **15**, 167.

Fu, S., Jiang, W., Gao, X., Zeng, A., Cholger, D., Cannon, J., Chen, J. H., and Zheng, W. (2016). Aberrant adult neurogenesis in the subventricular zone-rostral migratory stream-olfactory bulb system following subchronic manganese exposure. *Toxicol. Sci.* **150**, 347–368.

Fu, S., Jiang, W., and Zheng, W. (2015b). Age-dependent increase of brain copper levels and expressions of copper regulatory proteins in the subventricular zone and choroid plexus. *Front. Mol. Neurosci.* **8**, 22.

Fu, S., O'Neal, S., Hong, L., Jiang, W., and Zheng, W. (2015a). Elevated adult neurogenesis in brain subventricular zone following in vivo manganese exposure: Roles of copper and DMT1. *Toxicol. Sci.* **143**, 482–498.

Fu, X., Zhang, Y., Jiang, W., Monnot, A. D., Bates, C. A., and Zheng, W. (2014). Regulation of copper transport crossing brain barrier systems by Cu-ATPases: Effect of manganese exposure. *Toxicol. Sci.* **139**, 432–451.

Gao, X., Deng-Bryant, Y., Cho, W., Carrico, K. M., Hall, E. D., and Chen, J. (2008). Selective death of newborn neurons in hippocampal dentate gyrus following moderate experimental traumatic brain injury. *J. Neurosci. Res.* **86**, 2258–2270.

Gao, X., and Chen, J. H. (2011). Mild traumatic brain injury results in extensive neuronal degeneration in the cerebral cortex. *J. Pathol. Exp. Neurol.* **70**, 183–191.

Gao, X., Deng, P., Xu, Z. C., and Chen, J. H. (2011). Moderate traumatic brain injury causes acute dendritic and synaptic degeneration in hippocampal dentate gyrus. *PLos One* **6**, e24566–e24566.

Gorski, J. A., Zeiler, S. R., Tamowski, S., and Jones, K. R. (2003). Brain-derived neurotrophic factor is required for the maintenance of cortical dendrites. *J. Neurosci.* **23**, 6856–6865.

Gunter, T. E., Gavin, C. E., Aschner, M., and Gunter, K. K. (2006). Speciation of manganese in cells and mitochondria: A search for the proximal cause of manganese eurotoxicity. *Neurotoxicology* **27**, 765–776.

Ha Mai, D., and Bondy, S. (2004). Oxidative basis of manganese neurotoxicity. *Ann. N. Y. Acad. Sci.* **1012**, 129–141.

Hodge, R. D., Kowalczyk, T. D., Wolf, S. A., Encinas, J. M., Rippey, C., Enikolopov, G., Kempermann, G., and Hevner, R. F. (2008). Intermediate progenitors in adult hippocampal neurogenesis: Tbr2 expression and coordinate regulation of neuronal output. *J. Neurosci.* **28**, 3707–3717.

Horch, H. W., and Katz, L. C. (2002). BDNF release from single cells elicits local dendritic growth in nearby neurons. *Nat. Neurosci.* **5**, 1177–1184.

Jiang, Y. M., Mo, X. A., Du, F. Q., Fu, X., Zhu, X. Y., Gao, H. Y., Xie, J. L., Liao, F. L., Pira, E., and Zheng, W. (2006). Effective treatment of manganese-induced occupational parkinsonism with p-aminosalicylic acid: A case of 17-year follow-up study. *J. Occup. Environ. Med.* **48**, 644–649.

Jiang, Y. M., Zheng, W., Long, L. L., Zhao, W. J., Li, X. R., Mo, X. A., Lu, J. P., Fu, X., Li, W. M., Liu, S. T., *et al.* (2007). Brain magnetic resonance imaging and manganese concentrations in red blood cells of smelting workers: Search for biomarkers of manganese exposure. *Neurotoxicology* **28**, 126–135.

Jonas, P., and Lisman, J. (2014). Structure, function, and plasticity of hippocampal dentate gyrus microcircuits. *Front. Neural. Circuits* **8**, 107.

Kempermann, G., and Gage, F. H. (2000). Neurogenesis in the adult hippocampus. *Novartis Found. Symp.* **231**, 220–235. discussion 235–241, 302–226.

Kempermann, G., Song, H., and Gage, F. H. (2015). Neurogenesis in the adult hippocampus. *Cold Spring Harb. Perspect. Biol.* **7**, a018812.

Kikuchihara, Y., Abe, H., Tanaka, T., Kato, M., Wang, L., Ikarashi, Y., Yoshida, T., and Shibutani, M. (2015). Relationship between brain accumulation of manganese and aberration of hippocampal adult neurogenesis after oral exposure to manganese chloride in mice. *Toxicology* **331**, 24–34.

Latronico, T., Branà, M. T., Merra, E., Anna Fasano, A., Di Bari, G., Casalino, E., and Liuzzi, G. M. (2013). Impact of manganese neurotoxicity on MMP-9 production and superoxide dismutase activity in rat primary astrocytes. Effect of resveratrol and therapeutical implications for the treatment of CNS diseases. *Toxicol. Sci.* **135**, 218–228.

Liang, G. Q., Qin, H. Y., Zhang, L. E., Ma, S. Y., Huang, X. W., Lv, Y. N., Qing, L., Li, Q., Xiong, Y. X., Huang, Y. F., *et al.* (2015). Effects of chronic manganese exposure on the learning and memory of rats by observing the changes in the hippocampal cAMP signaling pathway. *Food Chem. Toxicol.* **83**, 261–267.

Liebner, S., Czupalla, C. J., and Wolburg, H. (2011). Current concepts of blood–brain barrier development. *Int. J. Dev. Biol.* **55**, 467–476.

Lois, C., and Alvarez-Buylla, A. (1994). Long-distance neuronal migration in the adult mammalian brain. *Science* **264**, 1145–1148.

Lucchini, R., Albini, E., Placidi, D., Gasparotti, R., Pigozzi, M. G., Montani, G., and Alessio, L. (2000). Brain magnetic resonance imaging and manganese exposure. *Neurotoxicology* **21**, 769–775.

Lv, Y., Zou, Y., Liu, J., Chen, K., Huang, D., Shen, Y., Zhong, Y., Liu, Z., Jiang, B., Li, Q., *et al.* (2014). Rationale, design and baseline results of the Guangxi manganese-exposed workers healthy cohort (GXMEWHC) study. *BMJ Open* **4**, e005070.

Menezes-Filho, J. A., Novaes, C. D. O., Moreira, J. C., Sarcinelli, P. N., and Mergler, D. (2011). Elevated manganese and cognitive performance in school-aged children and their mothers. *Environ. Res.* **111**, 156.

Miller, M. W., and Nowakowski, R. S. (1988). Use of bromodeoxyuridine-immunohistochemistry to examine the proliferation, migration and time of origin of cells in the central nervous system. *Brain Res.* **457**, 44–52.

Ming, G. L., and Song, H. (2005). Adult neurogenesis in the mammalian central nervous system. *Annu. Rev. Neurosci.* **28**, 223–250.

Montaron, M. F., Koehl, M., Lemaire, V., Drapeau, E., Abrous, D. N., and Le Moal, M. (2004). Environmentally induced long-term structural changes: Cues for functional orientation and vulnerabilities. *Neurotox. Res.* **6**, 571–580.

Morello, M., Canini, A., Mattioli, P., Sorge, R. P., Alimonti, A., Bocca, B., Forte, G., Martorana, A., Bernardi, G., and Sancesario, G. (2008). Sub-cellular localization of manganese in the basal ganglia of normal and manganese-treated rats An electron spectroscopy imaging and electron energy-loss spectroscopy study. *NeuroToxicology* **29**, 60–72.

Ohishi, T., Wang, L., Akane, H., Shiraki, A., Goto, K., Ikarashi, Y., Suzuki, K., Mitsumori, K., and Shibutani, M. (2012). Reversible aberration of neurogenesis affecting late-stage differentiation in the hippocampal dentate gyrus of rat offspring after maternal exposure to manganese chloride. *Reprod. Toxicol.* **34**, 408–419.

O'Neal, S. L., Hong, L., Fu, S., Jiang, W., Jones, A., Nie, L. H., and Zheng, W. (2014a). Manganese accumulation in bone following chronic exposure in rats: Steady-state concentration and half-life in bone. *Toxicol. Lett.* **229**, 93–100.

O'Neal, S. L., Lee, J. W., Zheng, W., and Cannon, J. R. (2014b). Subacute manganese exposure in rats is a neurochemical model of early manganese toxicity. *Neurotoxicology* **44**, 303–313.

Oner, G., and Sentürk, U. K. (1995). Reversibility of manganese-induced learning defect in rats. *Food Chem. Toxicol.* **33**, 559e563.

Palmer, T. D., Willhoite, A. R., and Gage, F. H. (2000). Vascular niche for adult hippocampal neurogenesis. *J. Comp. Neurol.* **425**, 479–494.

Parikh, V., Khan, M. M., and Mahadik, S. P. (2003). Differential effects of antipsychotics on expression of antioxidant enzymes and membrane lipid peroxidation in rat brain. *J. Psychiatr. Res.* **37**, 43–51.

Peres, T. V., Eyng, H., Lopes, S. C., Colle, D., Goncalves, F. M., Venske, D. K. R., Lopes, M. W., Ben, J., Bornhorst, J., Schwerdtle, T., *et al.* (2015). Developmental exposure to manganese induces lasting motor and cognitive impairment in rats. *NeuroToxicology* **50**, 28–37.

Pushkar, Y., Robison, G., Sullivan, B., Fu, S., Kohne, M., Jiang, W., Rohr, S., Lai, B., Marcus, M. A., Zakharova, T., *et al.* (2013). Aging results in copper accumulations in glial fibrillary acidic protein-positive cells in the subventricular zone. *Aging Cell* **12**, 823–832.

Racette, B. A., Aschner, M., Guilarte, T. R., Dydak, U., Criswell, S. R., and Zheng, W. (2012). Pathophysiology of manganese-associated neurotoxicity. *Neurotoxicology* **33**, 881–886.

Riojas-Rodríguez, H., Solís-Vivanco, R., Schilmann, A., Montes, S., Rodríguez, S., Ríos, C., and Rodríguez-Agudelo, Y. (2010). Intellectual function in Mexican children living in a mining area and environmentally exposed to manganese. *Environ. Health Perspect.* **118**, 1465–1465e1470.

Robison, G., Zakharova, T., Fu, X., Jiang, W., Fulper, R., Barrea, R., Marcus, M. A., Zheng, W., and Pushkar, Y. (2012). X-ray fluorescence imaging: A new tool for studying manganese neurotoxicity. *PLoS One* **7**, e48899.

Robison, G., Zakharova, T., Fu, S., Jiang, W., Fulper, R., Barrea, R., Zheng, W., and Pushkar, Y. (2013). X-ray fluorescence imaging of the hippocampal formation after manganese exposure. *Metallomics* **5**, 1554–1565.

Sarsour, E. H., Kalen, A. L., and Goswami, P. C. (2014). Manganese superoxide dismutase regulates a redox cycle within the cell cycle. *Antioxid. Redox Signal.* **20**, 1618–1627.

Sarsour, E. H., Venkataraman, S., Kalen, A. L., Oberley, L. W., and Goswami, P. C. (2008). Manganese superoxide dismutase activity regulates transition between quiescent and proliferative growth. *Aging Cell* **7**, 405–417.

Schneider, J. S., Williams, C., Ault, M., and Guilarte, T. R. (2013). Chronic manganese exposure impairs visuospatial associative learning in non-human primates. *Toxicol. Lett.* **221**, 146.

Seth, P. K., Husain, R., Mushtaq, M., and Chandra, S. V. (1977). Effect of manganese on neonatal rat: Manganese concentration and

enzymatic alteration in brain. *Acta Pharmacol. Toxicol.* **40**, 553–560.

Seth, P. K., Hong, J. S., Kilts, C. D., and Bondy, S. C. (1981). Alteration of cerebral neurotransmitter receptor function by exposure of rats to manganese. *Toxicol. Lett.* **9**, 247–254.

Shapiro, L. A., and Ribak, C. E. (2005). Integration of newly born dentate granule cells into adult brains: Hypotheses based on normal and epileptic rodents. *Brain Res. Brain Res. Rev.* **48**, 43–56.

Singh, J., Husain, R., Tandon, S. K., Seth, P. R., and Chandra, S. V. (1974). Biochemical and histopathological alterations in early manganese toxicity in rats. *Environ. Physiol. Biochem.* **4**, 16–23.

Smith, M. R., Fernandes, J., Go, Y. M., and Jones, D. P. (2017). Redox dynamics of manganese as a mitochondrial life-death switch. *Biochem. Biophys. Res. Commun.* **482**, 388–398.

Stansfield, K. H., Bichell, T. J., Bowman, A. B., and Guilarte, T. R. (2014). BDNF and Huntingtin protein modifications by manganese: Implications for striatal medium spiny neuron pathology in manganese neurotoxicity. *J. Neurochem.* **131**, 655–666.

Sumanont, Y., Murakami, Y., Tohda, M., Vajragupta, O., Watanabe, H., and Matsumoto, K. (2007). Effects of manganese complexes of curcumin and diacetylcurcumin on kainic acid-induced neurotoxic responses in the rat hippocampus. *Biol. Pharm. Bull.* **30**, 1732–1739.

Sutherland, R. J., Kolb, B., and Whishaw, I. Q. (1982). Spatial mapping: Definitive disruption by hippocampal or medial frontal cortical damage in the rat. *Neurosci. Lett.* **31**, 271.

Szpetnar, M., Luchowska-Kocot, D., Boguszewska-Czubara, A., and Kurzepa, J. (2016). The influence of manganese and glutamine intake on antioxidants and neurotransmitter amino acids levels in rats' brain. *Neurochem. Res.* **41**, 2129–2139.

Taupin, P. (2007). BrdU immunohistochemistry for studying adult neurogenesis: Paradigms, pitfalls, limitations, and validation. *Brain Res. Rev.* **53**, 198–214.

Tolwani, R. J., Buckmaster, P. S., Varma, S., Cosgaya, J. M., Wu, Y., Suri, C., and Shooter, E. M. (2002). BDNF overexpression increases dendrite complexity in hippocampal dentate gyrus. *Neuroscience* **114**, 795–805.

Tong, M., Dong, M., and de la Monte, S. M. (2009). Brain insulinlike growth factor and neurotrophin resistance in Parkinson's disease and dementia with Lewy bodies: Potential role of manganese neurotoxicity. *J. Alzheimers Dis.* **16**, 5858–5599.

Verina, T., Kiihl, S. F., Schneider, J. S., and Guilarte, T. R. (2011). Manganese exposure induces microglia activation and dystrophy in the substantia nigra of non-human primates. *Neurotoxicology* **32**, 215–226.

Vigers, A. J., Amin, D. S., Talley-Farnham, T., Gorski, J. A., Xu, B., and Jones, K. R. (2012). Sustained expression of brainderived neurotrophic factor is required for maintenance of dendritic spines and normal behavior. *Neuroscience* **212**, 1–18.

Von Bohlen Und Halbach, O. (2007). Immunohistological markers for staging neurogenesis in adult hippocampus. *Cell Tissue Res.* **329**, 409–420.

Wang, L., Chang, X., She, L., Xu, D., Huang, W., and Poo, M. M. (2015). Autocrine action of BDNF on dendrite development of adult-born hippocampal neurons. *J. Neurosci.* **35**, 8384–8393.

Wang, L., Ohishi, T., Shiraki, A., Morita, R., Akane, H., Ikarashi, Y., Mitsumori, K., and Shibutani, M. (2012). Developmental exposure to manganese chloride induces sustained aberration of neurogenesis in the hippocampal dentate gyrus of mice. *Toxicol. Sci.* **127**, 508–521.

Wang, L., Shiraki, A., Itahashi, M., Akane, H., Abe, J., Mitsumori, K., and Shibutani, M. (2013). Aberration in epigenetic gene regulation in hippocampal neurogenesis by developmental exposure to manganese chloride in mice. *Toxicol. Sci.* **136**, 154–165.

Wedler, F. C., Denman, R. B., and Roby, W. G. (1982). Glutamine-synthetase from ovine brain is a manganese(II) enzyme. *Biochemistry* **21**, 6389–6396.

Wedler, F. C., and Denman, R. B. (1984). Glutamin-synthetase - the major Mn(II) enzyme in mammalian brain. *Curr. Top. Cell. Regul.* **24**, 153–169.

Wedler, F. C., Ley, B.W., and Grippo, A.A. (1989). Manganese(II) dynamics and distribution in glial cells cultured from chick cerebral cortex. *Neurochem Res.* **14**(11): 1129–1135.

Zhang, S., Fu, J., and Zhou, Z. (2004). In vitro effect of manganese chloride exposure on reactive oxygen species generation and respiratory chain complexes activities of mitochondria isolated from rat brain. *Toxicol. In Vitro* **18**, 71–77.

Zhao, F., Cai, T., Liu, M., Zheng, G., Luo, W., and Chen, J. (2009). Manganese induces dopaminergic neurodegeneration via microglial activation in a rat model of manganism. *Toxicol. Sci.* **107**, 156–164.

Zhao, C., Teng, E. M., Summers Jr, R. G., Ming, G. L., and Gage, F. H. (2006). Distinct morphological stages of dentate granule neuron maturation in the adult mouse hippocampus. *J. Neurosci.* **26**, 3–11.

Zheng, W., Jiang, Y. M., Zhang, Y., Jiang, W., Wang, X., and Cowan, D. M. (2009). Chelation therapy of manganese intoxication with para-aminosalicylic acid (PAS) in SpragueDawley rats. *Neurotoxicology* **30**, 240–248.

Zheng, W., Kim, H., and Zhao, Q. (2000). Comparative toxicokinetics of manganese choloride and methylcyclopentadienyl manganese tricarbonyl (MMT) in Sprague-Dawley rats. *Toxciol. Sci.* **54**, 295–301.

Zheng, W., Ren, S., and Graziano, J. H. (1998). Manganese inhibits mitochondrial aconitase: A mechanism of manganese neurotoxicity. *Brain Res.* **799**, 334–342.

Zou, Y., Qing, L., Zeng, X., Shen, Y., Zhong, Y., Liu, J., Li, Q., Chen, K., Lv, Y., Huang, D., *et al.* (2014). Cognitive function and plasma BDNF levels among manganese-exposed smelters. *Occup. Environ. Med.* **71**, 189–189e194.